# Characterization of Dielectric Properties of Nematic Liquid Crystals Using an Optically-Transparent Microstrip Resonator at 5 GHz


Bradley C. Mee
*Dept. of Engineering Science*
*University of Oxford*
Oxford, OX1 3PJ, UK
bradley.mee@eng.ox.ac.uk

Steve J. Elston
*Dept. of Engineering Science*
*University of Oxford*
Oxford, OX1 3PJ, UK
steve.elston@eng.ox.ac.uk

Stephen M. Morris
*Dept. of Engineering Science*
*University of Oxford*
Oxford, OX1 3PJ, UK
stephen.morris@eng.ox.ac.uk

Justin P. Coon
*Dept. of Engineering Science*
*University of Oxford*
Oxford, OX1 3PJ, UK
justin.coon@eng.ox.ac.uk



***Abstract*—This work reports the design, simulation, and fabrication of an optically-transparent microstrip line resonator that is employed to characterize the dielectric properties of a nematic liquid crystal (LC) at a frequency of 5 GHz, to understand the behaviour of LC-based optically-transparent radio frequency devices, and to allow direct observations of the LC through a polarising optical microscope while operating the device. The microstrip line is constructed by etching indium tin oxide (ITO)-coated glass and exploiting the first-order resonance to infer the anisotropic dielectric properties of the nematic LC. Results are compared with a microstrip line device featuring the same geometry but constructed from FR-4 and copper, and full-wave electromagnetic simulations that suggest an accuracy of 95% in the LC dielectric properties.**



***Index Terms*—Dielectric measurements; nematic liquid crystal; optically transparent devices; microstrip line;**


## I. Introduction

Thermotropic liquid crystals (LCs) exhibit properties of both isotropic liquids and crystalline solid states, within a certain temperature range. The nematic mesophase is defined by a scalar order parameter, *S*, where $S = 1$ and $S = 0$ relate the ideally ordered crystalline and isotropic states, respectively; a nematic LC typically exists in the range $0.3 < S < 0.8$. An important property of LCs is the dielectric anisotropy, which can be exploited using an applied electric field to alter the orientation of the director (the average pointing direction of the molecules). This anisotropy has long been exploited at optical wavelengths, for example in display technology, but has recently been considered for use in the radio frequency (RF) band to produce reconfigurable devices, e.g., antennas [1] or phased arrays [2].

Knowledge of the LC permittivity is therefore essential to understand the operation of these RF-LC devices. Erstwhile development of these reconfigurable antennas, or dielectric characterization of LCs [3], [4], focused on traditional materials for PCBs, such as copper and FR-4. However, recent works have sought to develop optically-transparent patch antennas, using indium tin oxide (ITO), or metal meshes (MMs), on glass substrates to produce devices that are transparent at optical wavelengths but remain conductive at RF, i.e., $1-100$ GHz. In [5], a nematic LC was utilized to produce an optically-transparent reconfigurable antenna, while in [6] a transparent phased array with nematic LC was considered. In both of these cases, the effective dielectric permittivity of the device was unknown: all previous work on characterizing LC dielectric properties have employed a traditional substrate/conductor material. It is also desirable to observe the LC alignment under a polarising optical microscope (POM): this was not possible when using FR-4 devices to infer dielectric properties, but can be achieved with ITO/glass microstrips.

Here, the development of a microstrip line device that is optically-transparent will be employed to characterize a nematic LC at 5 GHz to aid the understanding of optically-transparent RF-LC devices, and observe the alignment of the LC while under measurement. This measurement will be benchmarked against full-wave electromagnetic simulations and a microstrip device constructed with FR-4/copper using the same geometry. Background theory is discussed in Section II, with device fabrication in Section III. Measurement and simulation results are presented in Section IV before concluding the work.

## II. Background

### A. Liquid Crystals

Calamitic nematic LCs consist of long, rod-like molecules that have no long-range positional order but do exhibit an average orientational order, which is the preferred direction of the long molecular axis, known as the LC director and denoted by the unit vector **n**, as illustrated in Fig. 1. For a uniaxial, calamitic nematic LC, the symmetry exhibited simplifies the second-rank permittivity tensor to

$$\left[\bar{\varepsilon}\right] = \begin{bmatrix} \varepsilon_{r,\perp} & 0 & 0 \\ 0 & \varepsilon_{r,\perp} & 0 \\ 0 & 0 & \varepsilon_{r,\parallel} \end{bmatrix} \cdot \varepsilon_0 \tag{1}$$

where $\varepsilon_0$ is the permittivity of free space, and $\varepsilon_{r,\perp}$ and $\varepsilon_{r,\parallel}$ refer to the relative dielectric permittivity measured perpendic-


B. C. M. gratefully acknowledges the EPSRC and Toshiba for an iCASE studentship, and the John Fell Fund.

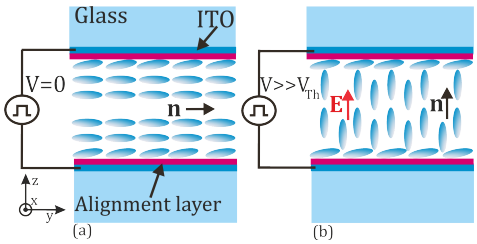


Fig. 1. When employing homogeneous alignment layers, and no applied voltage, the LC director will align horizontally through the bulk of the LC (a). Applying a voltage $V >> V_{Th}$ will align the director parallel to the field (b).

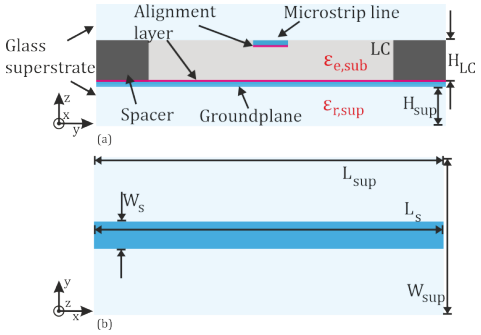


Fig. 2. Microstrip line geometry with end view in (a), and top view in (b).

ular and parallel to the director, respectively. Hence, an electric field applied along the positive $z$-direction would experience a different permittivity if the LC director was aligned along the $x$ or $y$-directions, given by $\varepsilon_{r,\perp}$, compared with if it was aligned along the $z$-direction i.e., $\varepsilon_{r,\parallel}$. The variation in relative dielectric permittivity, $\Delta\varepsilon_r$, is defined as

$$\Delta\varepsilon_r = \varepsilon_{r,\parallel} - \varepsilon_{r,\perp} \tag{2}$$

with the change in permittivity a continuum of values between the two ideally aligned states. The difference in permittivity may be positive or negative depending on the LC compound/mixture.

When unperturbed, the LC director aligns along the preferred axis, in the low energy state, until an external stimulus is applied such as an electric or magnetic field, illustrated in Fig. 1. For a nematic LC with positive dielectric anisotropy, an applied electric field that produces a voltage greater than the Fréedericksz threshold voltage, $V_{Th}$, will induce the LC director to begin to align parallel with the field [7]. Increasing the voltage $V >> V_{Th}$ will align the LC director parallel to the applied electric field. When then the electric field is removed, the LC director returns to the low energy state. Thus, controlling the LC director alters the relative dielectric permittivity of the LC, producing a continuously tunable material. For most nematic LCs $V_{Th} \approx 1$ V.

### B. Transparent Conductive Films

Doping indium oxide with tin oxide produces the transparent conductive film (TCF) semiconductor material known as ITO, which is transparent between wavelengths of 400 - 800 nm and electrically conductive. There is a trade-off required between electrical conductivity, in terms of sheet resistance and optical transparency: enhancing transparency leads to a deterioration of the sheet resistance. Furthermore, the thin films, typically of 100 – 500 nm in thickness, induce ohmic losses through the skin effect.

Nonetheless, ITO is advantageous due to its superior transparency, typically $> 90\%$ between wavelengths of 400 - 800 nm, over other TCFs or MMs, although the electrical conductivity is lower than that of copper, with $\sigma_{copper} \approx 6 \times 10^7$ S/m and $\sigma_{ITO} \approx 6 \times 10^5$ S/m [8]. ITO also provides full coverage over the substrate for the application of an electric field, whereas MM electrodes cover a minimal area and drastically reduce the regions where the LC can be stimulated.

## III. Experimental Methods

### A. Microstrip Design

A microstrip line device was employed due to its simple geometry for etching the ITO-coated glass, and analysis of its electrical properties. The resonant frequency, $F_r$, is

$$F_r = \frac{c}{2L\sqrt{\varepsilon_e}} \tag{3}$$

where $c$ is the speed of light in a vacuum, $L$ is the length of the conductive strip, and $\varepsilon_e$ is the effective permittivity of the substrate and surrounding material, here, the LC and glass superstrate, respectively. The effective permittivity can be related to the relative permittivity via conformal transformations to account for the interface between two materials using closed-form equations [9]. The microstrip line was constructed by etching ITO-coated glass, with a second piece of ITO-coated glass (unetched) providing the groundplane. Two 300 $\mu$m spacers were utilized to separate the two pieces of glass, into which a nematic LC was infiltrated. Hence, the device featured ITO as the conductive microstrip line and groundplane, separated by the LC acting as the dielectric substrate. For clarity, the glass will be termed as the superstrate and LC the substrate. The permittivity of the glass superstrate was measured at 4 GHz using a resonant technique. The geometry of the device is defined in Fig. 2 with values detailed in Table I.

To fabricate devices 1 and 2, Oscilla ITO-coated glass superstrates, 20 mm $\times$ 15 mm $\times$ 1.1 mm (length, width, height), with a 100 nm film of ITO covering one side of the glass, i.e., an area of 20 mm $\times$ 15, mm were utilized. The ITO was etched using a Trotec Speedy 360 laser engraving machine featuring a 130 W laser, with the laser power, speed, frequency and dots per inch (DPI) set as 5%, 5%, 1000 Hz and 500, respectively.

Device 3 was fabricated using a LPFK Protolaser to cut the microstrip geometry from copper-clad FR-4 board. The device was constructed in the same manner as devices 1 and 2.

TABLE I
MICROSTRIP LINE, SUBSTRATE AND LC PARAMETERS. DEVICE 1 AND 2 CORRESPOND TO GLASS/ITO AND DEVICE 3 CORRESPONDS TO FR-4/COPPER.

| Device | $L_s$ [mm] | $W_s$ [mm] | $H_{LC}$ [mm] | $W_{sup}$ [mm] | $L_{sup}$ [mm] | $H_{sup}$ [mm] | $\varepsilon_{r,sup}$ |
|---|---|---|---|---|---|---|---|
| 1 | 16 | 1.7 | 0.3 | 15 | 20 | 1.1 | 6.7 |
| 2 | 20 | 1.7 | 0.3 | 15 | 20 | 1.1 | 6.7 |
| 3 | 16 | 1.7 | 0.3 | 15 | 20 | 1.56 | 6.7 |

### B. Liquid Crystal Incorporation

A homogeneous alignment layer was achieved by depositing $1\%$ wt of polyvinyl alcohol (PVA) in distilled water, onto the conductive regions of both superstrates, i.e., the microstrip line and groundplane, spin-coating the sample and then applying a mechanical rubbing process to the PVA coated regions to produce the pre-tilt angle of $\approx 5°$. 300 $\mu$m spacers were attached to the groundplane and the two superstrates were fixed together by infiltrating UV-curable glue at the edges before curing in a UV oven for 10 minutes. The nematic LC mixture known as 'E7', sourced from Synthon Chemicals Ltd, was infiltrated between the groundplane and microstrip to act as the dielectric substrate of the microstrip device.

## IV. RESULTS

### A. ITO Etching

The results of the laser etching process described in Section III are portrayed in Fig. 3, by an image of the microstrip line (a) and under a microscope with $\times 4$ zoom (b). The features of the microstrip line are well delineated, with the average strip width 1750 $\mu$m. The glass underneath the regions where the ITO was removed was damaged and became opaque, although this was not a concern for this application.

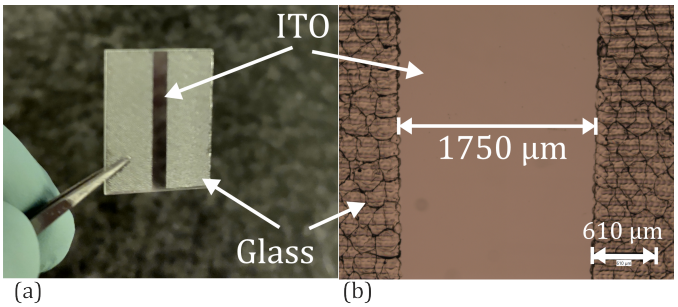


Fig. 3. Results of laser etching ITO from the glass. Image of the etched ITO (a) and viewed under a microscope at $\times 4$ magnification in (b).

### B. S-parameter Measurements

S-parameter measurements were conducted using a Rohde & Schwarz ZNB43 vector network analyzer (VNA), with a broadband bias tee (SHF BT45R) and DC-block (SHF DCB45R) inserted either side of the microstrip line device, shown in Fig. 4. The VNA was calibrated with the bias tee and DC-block attached to negate their effects on the measurement. A voltage generator was used to apply a 1 kHz square wave.

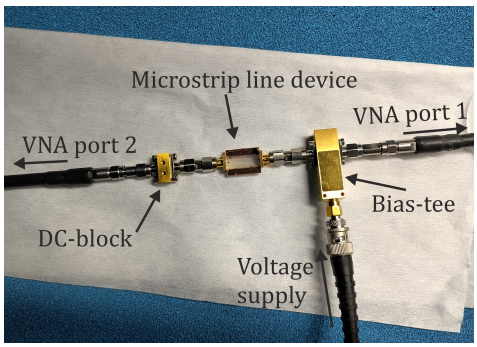


Fig. 4. Measurement of the S-parameters for the microstrip line device.

Measurement and simulation results for the first ITO-coated glass microstrip device, device 1 in Table I, are provided in Fig. 5. From the measurement results it is clear that applying the electric field over the LC region has indeed shifted the resonance frequency of the microstrip line. By observing the resonant frequency of the measured device at 0 V, Eqn. 3 was used to calculate the effective permittivity of the LC substrate, $\varepsilon_{e,\perp}$. The relative permittivity was then estimated by plotting closed-form equations in [9] over a range of values to find $\varepsilon_{r,\perp}$ graphically, however, this did not yield results that were reasonable based on previous dielectric permittivity measurements, e.g., in [4]. Hence, a range of values for $\varepsilon_r$ were trailed using CST simulations to find results congruent with the measurements, with results for these measurements, and comparison with other works detailed in II. The same process was thence applied to the resonant frequency of the device with 100 V to find $\varepsilon_{r,\parallel}$.

The $\tan\delta$ losses of the LC were estimated by $\tan\delta = 1/Q$, where $Q$ relates the Q-factor of each measured resonant point. The calculated values of $\tan\delta_\perp$ and $\tan\delta_\parallel$ were then input directly to the CST simulations, with further refinements made to match the measured results.

A second transparent microstrip line device was fabricated using the parameters detailed for device 2 in Table I, with the measurements results depicted in Fig. 6. There is a high degree of agreement, with results between the measured and simulated values accurate to within 2%. A third device was constructed, using the parameters for device 3 in Table I, with FR-4 and copper to compare the results with the ITO-coated glass devices. Again, simulated results are congruent with the measurements, to within 1%, and are displayed in Fig. 7.

Table II details the results for each device, including results from other published works. As the FR-4/copper device displayed high-quality resonance peaks at multiple modes, these results were included in Table II. The results for device 3 show excellent agreement with previous works that characterize the nematic LC 'E7'. The ITO-coated glass devices provided relative permittivity values that were in good agreement with other measured results, however, $\tan\delta$ losses were slightly higher. This was likely due to the lower conductivity and thickness of the ITO layer, compared to copper, causing additional losses that render the $\tan\delta = 1/Q$ assumption

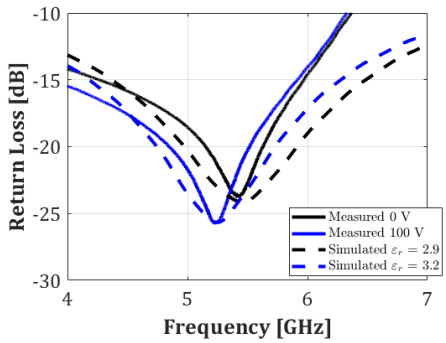


Fig. 5. Measured and simulated return loss for device 1.

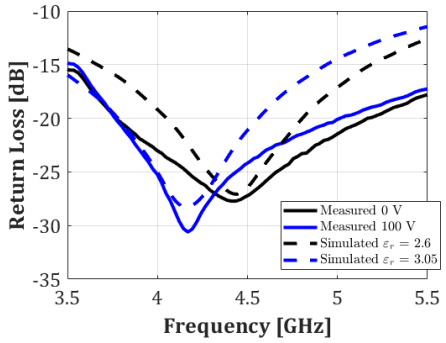


Fig. 6. Measured and simulated return loss for device 2.

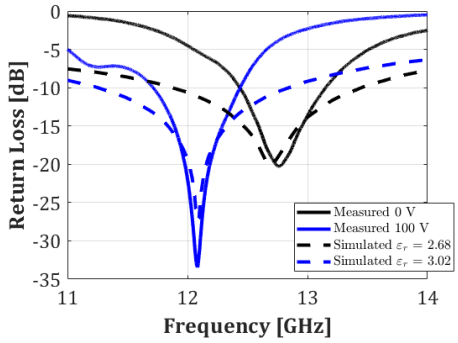


Fig. 7. Measured and simulated return loss for device 3.

as unreliable. Hence, these results suggest that closed-form equations for the permittivity and material losses cannot be applied to ITO-coated glass LC-based devices. Simulations of the E-fields reveal a reduction of 19.5% for E-field strength in the fringing fields of the microstrip line for the ITO/glass device, compared to the copper/FR4 device. This is likely the reason why the closed-form equations are incongruent with measurements, whereas EM simulations are agreeable.

## V. Conclusions

This work has detailed the design, fabrication, measurement and simulation of an optically-transparent microstrip line device to characterize the dielectric permittivity of a nematic LC, 'E7' at 5 GHz. Optically-transparent RF devices, such as antennas, utilize nematic LC in their fabrication, hence, it necessary to understand the effect on LC dielectric properties when incorporated with glass and ITO, compared to traditional devices. Accordingly, an FR-4 microstrip line device was constructed, with the same parameters as the transparent devices, to compare the results. Computer simulations of these devices suggest that the measurements are accurate to within 2%, providing reliable measurements to guide future design and fabrication of LC-based ITO/glass devices. Further work could develop closed-form equations to estimate the effective permittivity and material loses.

TABLE II
Measured properties for nematic LC 'E7', from this and other other published works.

| Device | $\varepsilon_{r,\perp}$ | $\varepsilon_{r,\parallel}$ | $\Delta\varepsilon_r$ | $\tan\delta_\perp$ | $\tan\delta_\parallel$ | $F_{r,\perp}$ [GHz] | $F_{r,\parallel}$ [GHz] |
|---|---|---|---|---|---|---|---|
| 1 | 2.9 | 3.2 | 0.3 | 0.071 | 0.63 | 5.4 | 5.24 |
| 2 | 2.6 | 3.05 | 0.45 | 0.02 | 0.005 | 4.41 | 4.17 |
| 3 | 2.16 | 2.46 | 0.3 | 0.032 | 0.034 | 6.37 | 5.9 |
| 3 | 2.68 | 3.02 | 0.34 | 0.019 | 0.034 | 12.7 | 12 |
| 3 | 2.63 | 3.1 | 0.35 | 0.017 | 0.014 | 18.76 | 17.46 |
| [4] | 2.18 | 2.62 | 0.44 | 0.039 | 0.012 | 4.32 | 4.06 |
| [10] | 2.87 | 3.11 | 0.24 | 0.05 | 0.02 | 3 | 3 |
| [11] | 2.69 | 3.12 | 0.43 | 0.036 | 0.015 | 5.14 | 4.8 |

## References


[1] B. C. Mee, S. M. Morris, J. P. Coon, *et al.*, "Reconfigurable bowtie antenna using a nematic liquid crystal," in *2023 IEEE Conference on Antenna Measurements and Applications (CAMA)*, 2023, pp. 507–512.

[2] W. Hu, R. Cahill, J. A. Encinar, *et al.*, "Design and measurement of reconfigurable millimeter wave reflectarray cells with nematic liquid crystal," *IEEE Transactions on Antennas and Propagation*, vol. 56, no. 10, pp. 3112–3117, 2008.

[3] P. Deo, L. Seddon, and *et al.*, "Microstrip device for broadband (15–65 ghz) measurement of dielectric properties of nematic liquid crystals," *IEEE Transactions on Microwave Theory and Techniques*, 2015.

[4] H. Peng, Y. Zhang, S. Zhu, M. Temiz, and A. El-Makadema, "Determining dielectric properties of nematic liquid crystals at microwave frequencies using inverted microstrip lines," *Liquid Crystals*, vol. 49, no. 15, pp. 2069–2081, 2022.

[5] B. C. Mee, W. Kamal, J. Ma, *et al.*, "Reconfigurable optically transparent antenna using drop-on-demand printed nematic liquid crystals," *In submission process*, 2024.

[6] P. Aghabeyki, P. de la Rosa, M. Caño-García, X. Quintana, R. Guirado, and S. Zhang, "Optically transparent beam-steering reflectarray antennas based on a liquid crystal for millimeter-wave applications," *IEEE Transactions on Antennas and Propagation*, vol. 72, no. 1, pp. 614–627, 2024.

[7] S. Chandrasekhar, *Liquid Crystals*, 2nd ed. Cambridge University Press, 1992.

[8] Z. J. Silva, C. R. Valenta, and G. D. Durgin, "Optically transparent antennas: A survey of transparent microwave conductor performance and applications," *IEEE Antennas and Propagation Magazine*, vol. 63, no. 1, pp. 27–39, 2021.

[9] I. Bahl, M. Bozzi, and R. Garg. 2013.

[10] H. Xu, O. Trushkevych, N. Collings, and W. A. Crossland, "Measurement of dielectric anisotropy of some liquid crystals for microwave applications," *Molecular Crystals and Liquid Crystals*, vol. 502, pp. 235–244, 2009.

[11] D. E. Schaub and D. R. Oliver, "A circular patch resonator for the measurement of microwave permittivity of nematic liquid crystal," *IEEE Transactions on Microwave Theory and Techniques*, vol. 59, no. 7, pp. 1855–1862, 2011.